Neuropsychopharmacology (2015) 40, 1037–1051

www.neuropsychopharmacology.org

Species Differences in Cannabinoid Receptor 2 and Receptor Responses to Cocaine Self-Administration in Mice and Rats

Hai-Ying Zhang[1], Guo-Hua Bi[1], Xia Li[1], Jie Li[1], Hong Qu[2], Shi-Jian Zhang[3], Chuan-Yun Li[3], Emmanuel S Onaivi[4], Eliot L Gardner[1], Zheng-Xiong Xi*,[1] and Qing-Rong Liu*,[5]

[1]Neuroropsychopharmacology Section, Molecular Targets and Medications Discovery Branch, Intramural Research Program, National Institute on Drug Abuse, Baltimore, MD, USA; [2]Center for Bioinformatics, College of Life Sciences, Peking University, Beijing, China; [3]Beijing Key Laboratory of Cardiometabolic Molecular Medicine, Institute of Molecular Medicine and Peking University, Beijing, China; [4]Department of Biology, William Paterson University, Wayne, NJ, USA; [5]Neurobiology of Relapse Section, Behavioral Neuroscience Research Branch, Intramural Research Program, National Institute on Drug Abuse, Baltimore, MD, USA

The discovery of functional cannabinoid receptors 2 (CB_2Rs) in brain suggests a potential new therapeutic target for neurological and psychiatric disorders. However, recent findings in experimental animals appear controversial. Here we report that there are significant species differences in CB_2R mRNA splicing and expression, protein sequences, and receptor responses to CB_2R ligands in mice and rats. Systemic administration of JWH133, a highly selective CB_2R agonist, significantly and dose-dependently inhibited intravenous cocaine self-administration under a fixed ratio (FR) schedule of reinforcement in mice, but not in rats. However, under a progressive ratio (PR) schedule of reinforcement, JWH133 significantly increased breakpoint for cocaine self-administration in rats, but decreased it in mice. To explore the possible reasons for these conflicting findings, we examined CB_2R gene expression and receptor structure in the brain. We found novel rat-specific CB_{2C} and CB_{2D} mRNA isoforms in addition to CB_{2A} and CB_{2B} mRNA isoforms. *In situ* hybridization RNAscope assays found higher levels of CB_2R mRNA in different brain regions and cell types in mice than in rats. By comparing CB_2R-encoding regions, we observed a premature stop codon in the mouse CB_2R gene that truncated 13 amino-acid residues including a functional autophosphorylation site in the intracellular C-terminus. These findings suggest that species differences in the splicing and expression of CB_2R genes and receptor structures may in part explain the different effects of CB_2R-selective ligands on cocaine self-administration in mice and rats.

Neuropsychopharmacology (2015) **40,** 1037–1051; doi:10.1038/npp.2014.297; published online 17 December 2014

INTRODUCTION

It was previously reported that the cannabinoid receptor 1 (CB_1R) is predominantly expressed in brain, whereas the cannabinoid receptor 2 (CB_2R) is predominantly expressed in the peripheral immune system (Matsuda, 1997). Therefore, the majority of CB_2R-related studies have focused on peripheral tissues. This view of central CB_1R and peripheral CB_2R cannabinoid systems has been challenged recently by growing evidence demonstrating functional CB_2R expression in brain (Atwood and Mackie, 2010; Mechoulam and Parker, 2013; Onaivi *et al*, 2012). Furthermore, the findings of neuronal CB_2Rs in the brain and their postsynaptic localization (Brusco *et al*, 2008a; Gong *et al*, 2006; Vinckenbosch *et al*, 2006) suggest an important role of the CB_2R in neuronal synaptic transmission and CNS disorders such as drug abuse, schizophrenia, and stroke (Onaivi *et al*, 2008; Onaivi *et al*, 2012).

However, neuronal localization of CB_2Rs in the brain has been controversial (Atwood and Mackie, 2010; Van Sickle *et al*, 2005) because of concerns regarding antibody specificities. Several independent groups have demonstrated a functional role for brain CB_2Rs in terms of genetic association with psychiatric diseases (Ishiguro *et al*, 2010a, b), cellular distributions and neuronal localizations (Lanciego *et al*, 2011; Suárez *et al*, 2009; Van Sickle *et al*, 2005), electrophysiological effects (den Boon *et al*, 2012; Morgan *et al*, 2009), and behavioral pharmacological effects using CB_2R transgenic mice (Callén *et al*, 2012; Garcia-Gutiérrez and Manzanares, 2011; Garcia-Gutiérrez *et al*, 2013; Navarrete *et al*, 2013; Xi *et al*, 2011). Strikingly, growing evidence demonstrates that brain CB_2Rs may be involved in drug reward and addiction. Xi *et al* (2011) recently reported that systemic or intracranial local administration of JWH133, a selective CB_2R agonist, into the nucleus

*Correspondence: Dr Z-X Xi Neuroropsychopharmacology Section, Molecular Targets and Medications Discovery Branch, Intramural Research Program, National Institute on Drug Abuse, Baltimore, MD 21224, USA, Tel: +1 443 740 2517, Fax: +1 443 740 2781, E-mail: zxi@intra.nida.nih.gov or Dr Q-R Liu Neurobiology of Relapse Section, Behavioral Neuroscience Research Branch, Intramural Research Program, National Institute on Drug Abuse, Baltimore, MD 21224, USA, Tel: +1 443 740 2731, Fax: +1 443 740 2827, E-mail: qliu@intra.nida.nih.gov
Received 3 July 2014; revised 23 October 2014; accepted 25 October 2014; accepted article preview online 6 November 2014

accumbens significantly inhibits intravenous (i.v.) cocaine self-administration in wild-type (WT) and CB_1R-knockout (CB_1-KO) mice, but not in CB_2-KO mice. Consistent with these findings, systemic administration of the CB_2R agonist O-1966 inhibits cocaine-induced conditioned place preference (CPP) in WT mice, but not in CB_2R-KO mice (Ignatowska-Jankowska *et al*, 2013). Transgenic mice with overexpression of CB_2R in the brain show decreased cocaine self-administration and cocaine-enhanced locomotion (Aracil-Fernández *et al*, 2012). In addition, systemic administration of the CB_2R agonist β-caryophyllene reduced voluntary alcohol intake, alcohol-induced CPP, and locomotor sensitization in mice (Al Mansouri *et al*, 2014). In contrast to the above findings, CB_2Rs appear to play an opposite role in mediating nicotine's action. It was reported that genetic deletion of CB_2Rs in mice attenuated nicotine self-administration (Navarrete *et al*, 2013) and abolished nicotine-induced CPP (Ignatowska-Jankowska *et al*, 2013). Congruently, pharmacological blockade of CB_2Rs by SR 144528 attenuates nicotine-induced CPP in WT mice (Ignatowska-Jankowska *et al*, 2013).

In contrast to the above findings in mice, the results with CB_2R ligands in rats appear controversial. Blanco-Calvo *et al* (2014) recently reported that pharmacological blockade of CB_1Rs (by SR144176A) or CB_2Rs (by AM630) prevents both cocaine-induced conditioned locomotion and cocaine-induced reduction of cell proliferation in the hippocampus of rats. Adamczyk *et al* (2012) reported that systemic administration of the CB_2R antagonist SR144528 had no effect on i.v. cocaine self-administration, but attenuated cocaine-induced reinstatement of drug-seeking behavior in rats. Furthermore, Gamaleddin *et al* (2012b) reported that systemic administration of the CB_2R agonist AM1241 or the antagonist AM630 does not alter nicotine self-administration or nicotine- or cue-induced reinstatement of nicotine-seeking behavior. The reasons underlying such conflicting findings are unclear. The simplest explanation may relate to different drugs of abuse (cocaine *versus* nicotine), different CB_2R agonists (JWH133 *versus* AM1241 or O-1966) or antagonists (AM630 *versus* SR144528), different drug doses, different species of animals, and different measures in different animal models.

In this study, we explored whether the above-noted different effects in addiction-related models may be related to species differences in CB_2R gene and receptor expression. To this end, we studied different effects of the CB_2R agonist JWH133 on cocaine self-administration in rats and mice. We then carried out a series of experiments to study and compare CB_2R gene structure and alternative splicing, CB_2R mRNA expression, and CB_2R amino-acid sequences and their 3D structures in mice and rats.

MATERIALS AND METHODS

Animal Subjects

Male Long–Evans rats (Charles River, Raleigh, NC) and WT and CB_2-KO mice with C57BL/6J genetic backgrounds (Buckley *et al*, 2000) were used in cocaine self-administration experiments. WT and CB_2-KO mice were bred within the Transgenic Animal Breeding Facility of the National Institute on Drug Abuse (NIDA). They were housed in a fully accredited animal facility and were maintained on a reversed 12 h light/dark cycle (lights on at 1900 h and lights off at 0700 h) with food and water available *ad libitum* in the home cage. The experimental procedures followed the Guide for the Care and Use of Laboratory Animals (1996) and were approved by the NIDA Animal Care and Use Committee.

Intravenous Cocaine Self-Administration

Surgery. Animals were prepared for i.v. cocaine self-administration by surgical catheterization of the right external jugular vein. The jugular catheters were constructed of microrenathane (Braintree Scientific, Braintree, MA), and catheterization was performed under sodium pentobarbital anesthesia using standard aseptic surgical techniques as described previously (Xi *et al*, 2011; Song *et al*, 2012; Xi *et al*, 2005). The self-administration cannulae were fixed to the skull with 4 stainless steel jeweler's screws (Small Parts, Miami Lakes, FL) and dental acrylic cement. During experimental sessions, each catheter was connected to an injection pump via tubing encased in a protective metal spring from the head-mounted connector to the top of the experimental chamber. To help prevent clogging, the catheters were flushed daily with a gentamicin–heparin saline solution (0.1 mg/ml gentamicin and 30 IU/ml heparin; ICN Biochemicals, Cleveland, OH).

Self-administration apparatus. Intravenous self-administration experiments were conducted in operant response test chambers (Model ENV-008CT for rats; Model ENV-307A for mice) from Med Associates (Georgia, VT). Each test chamber had two levers: one active and one inactive. Depression of the active lever activated the infusion pump; depression of the inactive lever was counted but had no consequence. A cue light and a speaker were located 12 cm above the active lever. The house light was turned on at the start of each 3 h test session. Scheduling of experimental events and data collection was accomplished using Med Associates software.

Self-administration procedure. After recovery from surgery, each rat or mouse was placed into a test chamber (day time—dark phase) and allowed to lever-press for i.v. cocaine (1 mg/kg/infusion) delivered in 0.08 ml or 0.01 ml over 4.6 s in rats and mice, respectively, on a fixed ratio 1 (FR1) reinforcement schedule. Each cocaine infusion was associated with presentation of a stimulus light and tone. During the 4.6 s infusion time, additional responses on the active lever were recorded but did not lead to additional infusions. Each session lasted 3 h. FR1 reinforcement was used for 3–5 days until stable cocaine self-administration was established: a minimum of 20 presses on the active lever per test session and stability criteria of $<15\%$ variability in interresponse interval, $<15\%$ variability in number of infusions taken, and $<15\%$ variability in number of presses on the active lever for at least 3 consecutive days. Subjects were then allowed to continue cocaine self-administration (0.5 mg/kg/infusion) under FR2 reinforcement. This dose of cocaine was chosen based on previous studies showing that it lies within the middle range of the descending limb of the cocaine dose–-response self-administration curve, where reliable dose-dependent effects are observed (Xi *et al*, 2005). To avoid cocaine overdose, each animal was limited to a maximum of 50 cocaine injections per 3 h session.

Effects of JWH133 on cocaine self-administration. We first evaluated the effects of systemic administration of JWH133 (10 and 20 mg/kg, i.p., 30 min before testing) or vehicle (Tocrisolve-100) on FR2 cocaine self-administration in one group of rats and one group of mice (within-subjects design, $n = 6$ rats/group and $n = 9$ mice/group). The doses of JWH133 were based on our previous work (Xi *et al*, 2011).

Cocaine self-administration under progressive ratio (PR) reinforcement. Initial cocaine self-administration under FR1 and FR2 reinforcement was identical to that outlined above. After stable cocaine self-administration under FR2 reinforcement was established, the subjects were switched to cocaine (0.5 mg/kg/injection) self-administration under a PR schedule, during which the work requirement (lever presses) needed to receive a single i.v. cocaine infusion was progressively raised within each test session (Xi *et al*, 2005) according to the following PR series: 1, 2, 4, 6, 9, 12, 15, 20, 25, 32, 40, 50, 62, 77, 95, 118, 145, 178, 219, 268, 328, 402, 492, and 603 until breakpoint (BP) was reached. BP was defined as the maximal work load (lever presses) completed for a cocaine infusion before a 1-h period during which no infusion was obtained by the animal. The PR schedule is computer programmed to progress to a maximum of 603 and the average BP was ~ 150. Animals were allowed to continue daily sessions of cocaine self-administration under PR reinforcement conditions until day-to-day variability in BP was within 1–2 ratio increments for three consecutive days. Once a stable BP was established, subjects were assigned to three subgroups to determine the effects of three different doses of JWH133 (0, 10, and 20 mg/kg, i.p.) on PR BP for cocaine self-administration. Additional groups of animals were used to observe the effects of intranasal administration of JWH133 (0, 10, 25, or 50 μg/side) on PR cocaine self-administration. Intranasal drug administration was performed under inhalant isoflurane anesthesia using the Fluovac System (Harvard Apparatus, Holliston, MA). We chose between-subjects design for this experiment because it is relatively difficult to re-establish stable BP cocaine self-administration after each test under PR reinforcement as compared with cocaine self-administration under FR2 conditions.

Oral Sucrose Self-Administration

The procedures for oral sucrose self-administration testing were identical to the procedures used for cocaine self-administration, except for the following: (1) no surgery was carried out in this experiment; and (2) active lever presses led to delivery of 0.1 ml of 5% sucrose solution into a liquid food tray on the operant chamber wall. The effects of JWH133 (same doses as in previous experiments) on oral sucrose self-administration maintained under FR2 reinforcement were evaluated.

RT-PCR Analysis of CB_2R Isoforms

Male Sprague–Dawley rats and WT and CB_2-KO mice on C57BL/6J genetic background (Charles River) were decapitated, and the brains were rapidly removed and frozen in $-50\,^{\circ}C$ isopentane solution, and then stored at $-80\,^{\circ}C$ freezer until for assays. Punches (12 gauge needle) of brain regions were taken from 1 mm coronal sections cut using a cryostat at $-20\,^{\circ}C$. Total rodent RNAs were isolated using the TRIzol Reagent. RNA integrity numbers (RINs) were >8 measured by Agilent 2100 Bioanalyzer (Agilent Technologies, Santa Clara, CA) for rat and mouse RNAs. Single-strand cDNAs were synthesized using the Superscript III first-strand cDNA synthesis kit according to the manufacturer's protocols (Invitrogen, Life Technologies, Carlsbad, CA). TaqMan probes (Figure 1 and Table 1) were designed using Primer Express 3.0 (Applied Biosystems, Life Technologies, Carlsbad, CA) at the splicing junctions of the different rat and mouse CB_2R isoforms. The endogenous control TaqMan probes were rat VIC-labeled GAPDH (ABI Cat. no. 4352338E) and mouse rat VIC-labeled β-actin (ABI Cat. no. 4352341E). Duplex PCR assays containing both the target and endogenous control TaqMan probes were carried out with Advanced TaqMan Fast Universal PCR Master Mix in a 7500 Fast TaqMan instrument using a default thermocycling program. For rCB_{2D} isoform expression analysis, SYBR green assay was carried out with primers designed across the intraexonic splicing site that produce PCR fragments with 223 bp representing spliced rCB_{2D} isoform. Quantification of real-time PCR was carried out as described previously with duplexed PCR and technical duplicates (Liu *et al*, 2009). Regular PCR was carried out by 9700 ThermoCycler and the amplification products were analyzed in 1% and 3% agarose gel stained with ethidium bromide. Various tissues of WT and a C-terminal-deleted partial knockout strain (Buckley *et al*, 2000) were used for PCR amplification. The amplified PCR bands were cut from the agarose gel and DNA extracted by Qiagen gel extraction kit. The purified PCR fragments were cloned into TA cloning vector (PCR4 Topo, Invitrogen Life Technology) and sequenced by Sanger sequencing method (SeqWright Genomic Services, Houston, TX). RNA-Seq data in human, rhesus macaque, mouse, and rat were downloaded and processed to verify the splice structure of CB_2R isoforms, according to standardized pipelines as reported previously (Zhang *et al*, 2014a).

RNAscope *In Situ* Hybridization (ISH)

Rat and mouse CB_2R RNAscope probes in C1 channel were custom made by Advanced Cell Diagnostics (ACD, Hayward, CA). Customer probes using 20 ZZ pairs for each target were synthesized according to $3'-$untranslated regions (UTRs) of rat rCB_2R (NM_001164143.2; 1935–2843) or mouse mCB_2R (NM_009924.3; 1877–2820). Catalog probes of mouse tyrosine hydroxylase (TH) and rat dopamine transporter (DAT) were ordered from ACD.

Rat or mouse brains were rapidly frozen in 100 ml $-50\,^{\circ}C$ isopentane. The frozen brains were sealed in zipper plastic bag, wrapped in labeled aluminum foil, and stored at $-80\,^{\circ}C$. Before ISH, brains were placed in a cryostat (CM 3050S) at $-20\,^{\circ}C$ for 2 h to allow for temperature equilibration and then sliced and trimmed to the desired coronal plane. The coronal sections were cut at 12 μm thickness using anti-rolling plate to flatten the section. The

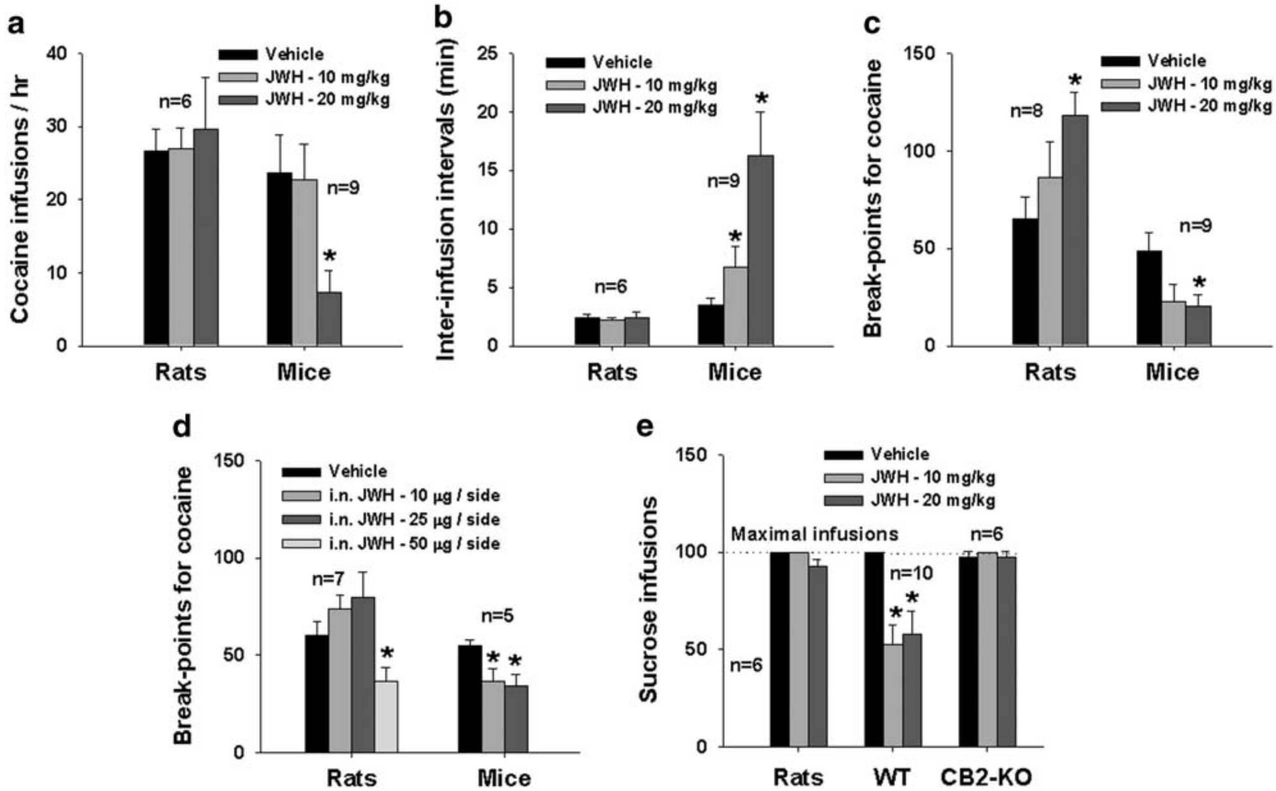

Figure 1 Differential effects of JWH133 on cocaine self-administration in rats and mice. (a) Systemic administration (i.p.) of JWH133 significantly decreased cocaine self-administration under fixed ratio (FR2) reinforcement in mice, but not in rats, as assessed by mean numbers of cocaine infusions per hour. (b) Systemic administration of JWH133 significantly increased interinfusion intervals in mice, but not in rats. (c) Systemic administration of JWH133 significantly increased PR BP for cocaine self-administration in rats, but decreased PR BP in mice. (d) Intranasal (i.n.) administration of JWH133 (10, 25, or 50 μg/10 μl/side) produced biphasic effects—low doses increased whereas high doses decreased PR BP in rats. (e) Systemic administration of JWH133 significantly inhibited oral sucrose self-administration in WT mice, but not in rats or CB_2-KO mice. *$P<0.05$, compared with vehicle control group.

Table 1 The qPCR Primer and TaqMan Probes for CB_2R Isoforms

Isoforms	TaqMan probe (5′–3′)	Forward primer (5′–3′)	Reverse primer (5′–3′)
mCB_{2A}	CTGACAAATGACACCCAGTC	CAGGACAAGGCTCCACAAGAC	GATGGGCTTTGGCTTCTTCTAC
mCB_{2B}	TGGGCCCAGTCTT	GCCACCCAGCAAACATCTCT	GATGGGCTTTGGCTTCTTCTAC
mCB_2-KO	ATGCTGGTTCCCTGCAC	AGCTCGGATGCGGCTAGAC	AGGCTGTGGCCCATGAGA
mCB_{2D}		CCCAAGGTCCTCGGTTACAGAAACA	CCCAACTCCTTCTGCTTATCCTTCA
rCB_{2A}	CTGACAAATGACTCCCAGTC	CAGGACAAGGCTTCACAAGAC	GACAGGCTTTGGCTGCTTCTAC
rCB_{2B}	TGGGCCCAGTCCT	GCCACCCAGCAAACATCTAT	GACAGGCTTTGGCTGCTTCTAC
rCB_{2C}	TGTCTGCAGCCACGC	CGGCTGACAAATGACTGAACAG	TGCCTACGCCTCTCCTCACT
rCB_{2D}		CCCAAAGTCCTCAGTTACAGAGACA	CCCAACTCCTGCTTATCCTTCA
rCB_2R_{410}	AGGCTGAGACTCTGGTC	CCCAAAGTCCTCAGTTACAGAGACA	CCCAACTCCTGCTTATCCTTCA

objective temperature was set to $-18\,^{\circ}C$ and the chamber temperature to $-19\,^{\circ}C$. Supper Frost Plus slides (Fisher, Cat. no. 12-550-15) were used to pick up each thin section by flipping the slide upside down and allowing each brain section to stick to the slides. The sections were spread out evenly using gloved finger under each section. The slides were left at $-20\,^{\circ}C$ for 10 min and transferred to $-80\,^{\circ}C$ for storage. The fixation, protease pretreatment, probe hybridization, preamplification, amplification, and fluorescent labeling steps were carried out according to User Manual for Fresh Frozen Tissue (ACD).

Wide-field fluorescent images of ventral tegmental area (VTA), nucleus accumbens (NAC), prefrontal cortex (PFC), and dorsal striatum (DST) were captured using a QimagingExi Aqua camera (Biovision) attached to a Zeiss AXIO Imager M2 microscope using a $\times 40$ objective (Zeiss PLAN-APOCHROMAT, $NA=1.3$) with oil immersion. Images were deconvoluted with Huygens software (v3.7, Scientific Volume Imaging), pseudo-colored (CB_2R green, TH and DAT red, and DAPI blue), and color joined using iVision software (Liu *et al*, 2014). Image Processing and Analysis by Java (ImageJ, NIH) software was used to quantify mRNA signals in each individual cell.

Bioinformatics

Rat and mouse CB_2R genomic structures were analyzed by NCBI Map Viewer (http://www.ncbi.nlm.nih.gov/mapview/) and UCSC Genome Browser (http://genome.ucsc.edu/). The exon and intron junctions were defined by alignment of exons with genomic sequences using Sequencher 5.0 software (Gene Codes Corporation, Ann Arbor, MI). The NCBI Blastn suite was used to align nucleotide sequences of rat and mouse CB_2R EST and PCR fragment sequences. CB_2R peptide sequences were aligned using CLUSTALW software (http://www.ebi.ac.uk/Tools/msa/clustalw2/). The CB_2R functional sites were predicted by The Eukaryotic Linear Motif database (http://elm.eu.org/), N-glycosylation was predicted by NetNGlyc 1.0 (http://www.cbs.dtu.dk/services/NetNGlyc/), and phosphorylation sites were predicted by ExPaSyNetPhos 2.0 (http://www.cbs.dtu.dk/services/NetPhos/).

The CB_2R peptide sequences of rat and mouse were submitted to the automated comparative protein modeling server Swiss-Model (Arnold *et al*, 2006; Guex and Peitsch, 1997; Schwede *et al*, 2003) (http://swissmodel.expasy.org/) to build up three-dimensional (3D) structures using the crystal structure of turkey β-adrenergic receptor (PDB: 4ajm) as a modeling template. The 3D figures were created with PyMOL (http://www.pymol.org/).

GenBank accession numbers were submitted as follows: JN420349 for rat CB_{2C} and JX494784 for rat CB_{2D}.

Data Analysis

Data are presented as means ± SEM of cocaine infusions per hour, cocaine infusion intervals, and BPs in the absence or presence of JWH133 pretreatment. Two-way ANOVA (Graphpad Software v6.0) for repeated measures over JWH133 doses was used to determine the significance of JWH133 effects. Nonrepeated measures ANOVA over rats and mice were used to determine significances of the JWH133 effects on cocaine or sucrose self-administration.

Two brain sections of different brain regions from each of two mice or two rats were used for quantification of CB_2R mRNA in 6–8 cells per region. For VTA sections, mTH- or rDAT-positive and -negative cells were counted separately in order to quantify mCB_2R and rCB_2R in mice and rats, respectively. Pixels were used to quantify CB_2R mRNA in each individual cell and intensities were used to quantify CB_2R in dopamine and nondopamine cells of VTA. Regular two-way ANOVA was used for statistical analysis of species differences and mixed two-way ANOVA was used for analysis using dopamine and nondopamine cells as the within-subjects variable and mice and rats as the between-subjects variable. Multiple comparisons were corrected by the Sidak method included in the software. The corrected significance level was $p < 0.05$.

RESULTS

Differential Effects of JWH133 on Cocaine Self-Administration in Mice and Rats

Figure 1 shows the effects of JWH133 on cocaine and sucrose self-administration under fixed ratio 2 (FR2) or PR reinforcement in both rats and mice. Systemic administration of JWH133 (10 and 20 mg/kg) significantly inhibited i.v. cocaine self-administration under FR2 reinforcement, as indicated by decreased number of cocaine infusions per hour and increased intercocaine infusion intervals, in mice, but not in rats. Although two-way ANOVA for repeated measures for the cocaine infusion rate data (Figure 1a) did not reveal a statistically significant JWH133 treatment main effect ($F_{2,26} = 5.53$, $p > 0.05$), a statistically significant species main effect ($F_{1,13} = 3.58$, $p < 0.05$) and a JWH133 × species interaction ($F_{2,26} = 5.48$, $p = 0.01$) were revealed. Two-way ANOVA for the cocaine infusion interval data (Figure 1b) revealed a significant JWH133 treatment main effect ($F_{2,26} = 5.89$, $p < 0.01$), species main effect ($F_{1,13} = 14.91$, $p < 0.01$), and a JWH133 × species interaction ($F_{2,26} = 5.47$, $p = 0.01$). Figure 1c shows the effects of JWH133 on BP for i.v. cocaine self-administration in rats and mice, illustrating that JWH133, at the same doses (10 and 20 mg/kg, i.p.), significantly increased PR BP for cocaine self-administration in rats, but decreased it in mice. Again, although two-way ANOVA did not reveal a statistically significant JWH133 treatment main effect ($F_{2,52} = 1.15$, $p > 0.05$), a statistically significant species main effect ($F_{1,52} = 43.49$, $p < 0.001$) and a significant JWH133 × species interaction ($F_{2,52} = 11.6$, $p < 0.01$) were revealed.

To determine the mechanisms by which JWH133 produced opposite effects on PR cocaine self-administration in rats and mice, we hypothesized that an increase in PR BP for cocaine self-administration in rats may be a compensatory response to a partial reduction in cocaine's rewarding efficacy and, therefore, a high dose of JWH133 may be required to produce an inhibitory effect similar to that seen in mice. However, testing higher systemic doses of JWH133 (eg, > 20 mg/kg) is problematic because of unwanted side effects, particularly locomotor inhibition. Therefore, we used intranasal drug delivery route by which many drugs may enter brain directly (Costantino *et al*, 2007; Illum *et al*, 2002). Figure 1d shows that intranasal administration of JWH133 produced biphasic effects—lower doses (10 and 25 μg/side) increased whereas a higher dose (50 μg/side) decreased BP for cocaine self-administration in rats ($F_{3,18} = 8.89$, $p < 0.001$). However, in WT mice, intranasal administration of JWH133 (10 and 20 μg/side) produced a monophasic inhibition of cocaine self-administration ($F_{2,11} = 4.59$, $p < 0.05$).

To determine whether systemic administration of JWH133 also alters other reward-reinforced behavior, we observed the effects of JWH133 on oral sucrose self-administration in rats and mice. We found that JWH133 significantly inhibited sucrose self-administration in WT mice (Figure 1, $F_{2,18} = 13.09$, $p < 0.001$), but not in rats or in CB_2-KO mice (Figure 1e).

Different CB_2R mRNA Isoforms Found in Rats and Mice

Figure 2 shows rat CB_2 (rCB_2R) and mouse CB_2 (mCB_2R) receptor gene and transcript (mRNA) structures, illustrating

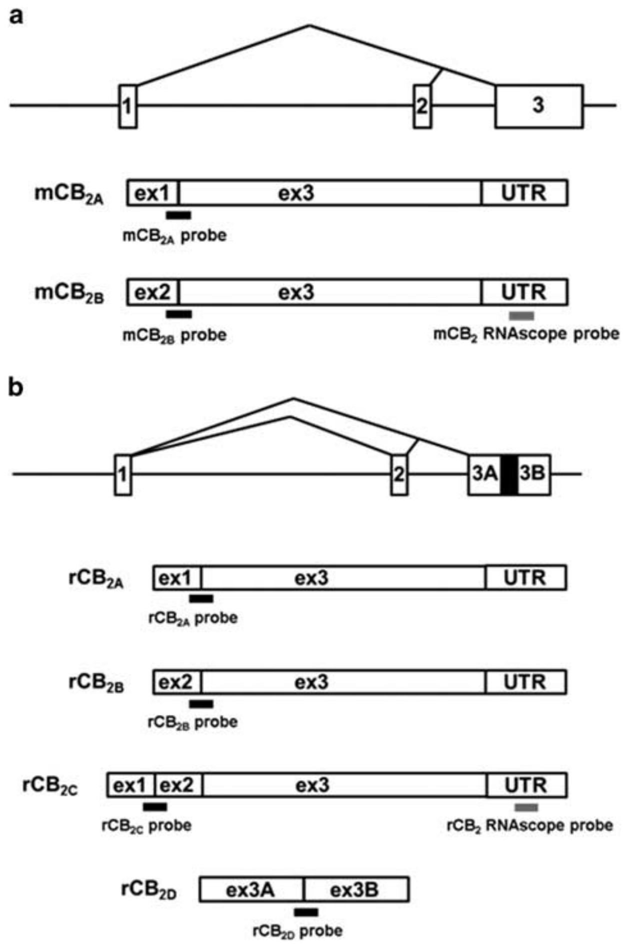

Figure 2 (a) Mouse CB_2 (mCB_2R, *Cnr2*, 4D3) and (b) rat CB_2 (rCB_2R, *Cnr2*, 5q36) genomic structures, alternatively spliced transcripts, and the locations that each probe targeted to detect brain CB_2 mRNA. Gene: open boxes represent exons, horizontal lines introns and black box mini-intron within the last exon. Transcripts: spliced exon numbers are indicated in the exons. The TaqMan probes were designed to fit the junctions of the spliced exons and are represented by horizontal black bars. The RNAscope probes hybridize 3′-UTR regions marked by gray boxes.

3 exons spanning ~25 kb, multiple CB_2R mRNA isoforms, and the splicing junction locations of probes that were used to detect different CB_2 mRNA isoforms. Using RT-PCR and DNA fragment agarose gel electrophoresis analysis, we detected CB_{2A} and CB_{2B} isoforms in both rats and mice, and CB_{2C} and CB_{2D} only in rats, but not in mice (Figure 3a–c). In this study, we used primers that targeted the conjunction region of exons 1–3 (94 bp) or exons 2 and 3 (85 bp) to detect CB_{2A} and CB_{2B} isoforms, respectively, in rat and mouse brain (Figure 3a and b). Unexpectedly, the CB_{2A} primers also detected an additional 189 bp RT-PCR fragment in rats, not in mice, suggesting a novel rCB_{2C}-specific isoform (Figure 3a). The sequence analysis of the PCR fragment of rCB_{2C} indicated that it was generated by exons 1–3 via interexonic tripartite exon splicing events. The rCB_{2D} was represented by a 223-bp RT-PCR fragment that was detected in amygdala, spleen, liver, and ovary tissues (Figure 3c). Sequence analysis of the PCR fragment of rCB_{2D} indicated that it was generated by intraexonic splicing of the third exon in the 3′-UTR (FJ496961: 1465–2252) with 786 bp deletion. Mouse brain and peripheral tissues neither expressed the corresponding 189 bp rCB_{2C} nor 233 bp rCB_{2D} PCR fragments (Figure 3a and c). Analysis of the RNA-Seq data in spleen also suggested the presence of rCB_{2C} and the absence of the corresponding mouse isoform (Zhang *et al*, 2013). Figure 3d shows that mCB_2 mRNA signal was detectable only in WT mice, but not in CB_2-KO mice (Figure 3dB and C), when using a probe that targeted the gene-deleted region in CB_2-KO mice (Figure 3dA). However, the probe targeted at CB_{2A} or CB_{2B} showed enhanced expression in various tissues of CB_2-KO mice, possibly because of compensatory effects after the partial C-terminal deletion in the CB_2-KO mouse strain (Buckley *et al*, 2000; Liu *et al*, 2009).

Quantitative PCR assay was carried out to compare expression of CB_2R isoforms in brain and peripheral tissues of rats and mice. We used cortex CB_2R mRNA level as a reference for brain expression and testis CB_2 mRNA level as a reference for peripheral expression because cortical or testis CB_2 mRNA levels are relatively the same in rats and mice. We found that the levels of CB_{2A} and CB_{2B} were higher in spleen (~100–600-fold) than in brain and testis (Figure 4a and b). However, the rat-specific isoform rCB_{2C} mRNA levels are relatively lower in spleen (approximately six fold; Figure 4c) whereas rCB_{2D} (Figure 4d) is predominantly expressed in spleen (~2000-fold) compared with rCB_{2A} and rCB_{2B} expression.

RNAscope ISH of CB_2R in Rat and Mouse Brains

We then further used an ultrasensitive RNAscope ISH method to detect and quantify low densities of CB_2R mRNA expression in brain slices of rats and mice, as the traditional ISH method may not be sensitive enough to detect the low levels of CB_2R mRNA in rodent brains (Tubbs *et al*, 2013; Wang *et al*, 2012). Figure 5a shows mouse and rat coronal atlas, illustrating PFC, VTA, DST, and NAC. Figure 5b and c show the quantitative analysis results. We used ImageJ software to count the pixels of CB_2R mRNA of 6–8 cells in 2 to 3 brain sections of each brain region and intensities of CB_2R mRNA in VTA dopamine (DA+) and nondopamine (DA−) cells. We observed that CB_2R mRNA pixels (2–25) in each cell were lowest in NAC and DST (2–5) and highest in VTA (20–25) in both rats and mice. Overall, more CB_2R mRNAs were found in each brain region in mice than in rats (Figure 5b, $F_{3,8}=46$, $p<0.001$). There was less CB_2R mRNA in DA neurons than those of non-DA neurons (Figure 5c, $F_{1,2}=678$, $p<0.01$) in rat VTA but no difference in mouse VTA. Figure 5d shows representative CB_2R mRNA staining using the RNAscope probes that hybridize to the 3′-UTR of CB_2R gene in mice (NM_009924, 1877–2820 bp, Figure 2a) and rats (NM_001164143, 1935–2843 bp, Figure 2b), illustrating CB_2 mRNA expression in each brain region. In the VTA, CB_2 mRNA was detectable in TH-positive or DAT-positive neurons, respectively, in mice and rats.

Species Differences in CB_2R Protein Structures

As there are no actual X-ray crystallographic structures of cannabinoid receptor CB_1R and CB_2R, we predicted 3D structures of rat and mouse CB_2Rs based on the structure of

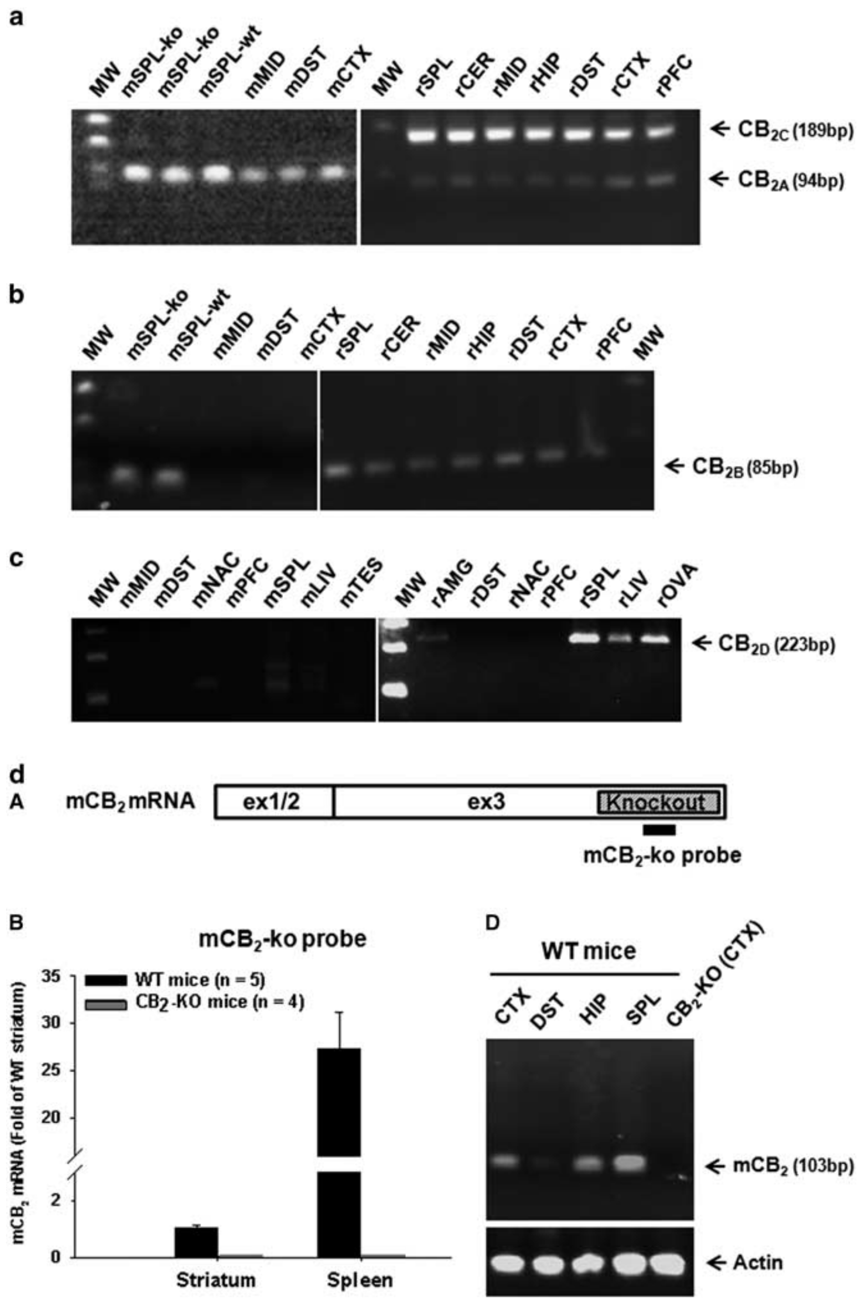

Figure 3 Agarose gel analysis results of PCR fragments, illustrating mCB_{2A}, rCB_{2A}, and rCB_{2C} (a), mCB_{2B} and rCB_{2B} (b), and rCB_{2D} (c) isoforms (ie, shown in Figure 2). When using a probe that targeted the gene-deleted region in CB_2-KO mice, mCB_2 mRNA signal was detectable only in the striatum and spleen of WT mice, but not in CB_2-KO mice (d). MW, molecular weight marker; SPL, spleen; ko-CB_2, knockout mice; wt, wild type; MID, midbrain; CTX, cortex; CER, cerebellum; HIP, hippocampus; PFC, prefrontal cortex; MID, midbrain; DST, dorsal striatum; NAC, nucleus accumbens; AMG, amygdala; LIV, liver; TES, testis; OVA, ovary; Prefix: m, mouse and r, rat.

turkey β-adrenergic receptor (residues 2–327; PDB ID code 4ajm, chain B) that shares amino-acid sequence identity of 23.5% (90/383) and similarity of 39.7% (152/383) with human hCB_2R. Figure 6 shows the predicted 3D structures of mCB_2R and rCB_2R (residues 27–315) with 7 transmembrane domains (TMs) and 3 extra- and 3 intracellular loops (ECL 1–3 and ICL 1–3). We drew the N- and C-terminus portions in both 3D and 2D models in order to show the truncated sequence in mouse CB_2R. The amino-acid sequences are highly conserved in the 7 TMs and less conserved in ECLs and ICLs. The acidic and basic amino-acid substitutions in ECLs and ICLs are marked by numbers and colored lines between rats and mice. The ligand-binding motifs of TM3-DRY (ionic lock) and TM7-NPXXY (water pocket) (Rosenbaum *et al*, 2009) and functional amino acids S112, D130, L201, Y207, and A244 (Feng and Song, 2003; Song and Feng, 2002; Tao *et al*, 1999) as well as important cysteine residues are completely conserved in primate and rodent CB_2Rs (Mercier *et al*, 2010). The proline residues in the TM regions involved in

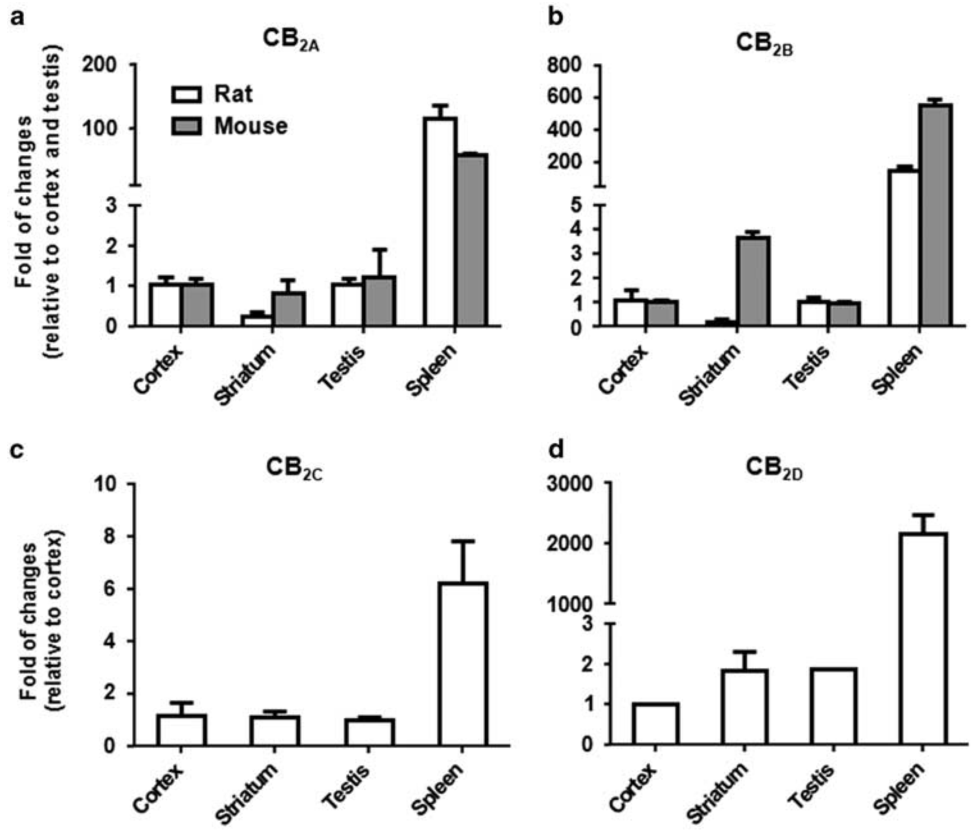

Figure 4 RT-qPCR comparison of CB_2R isoform tissue expression in mice and rats. The white bars represent rCB_2 mRNA levels in rat tissues and the gray bars represent mCB_2 mRNA levels in mouse tissues. The y axis is fold change in CB_2 mRNA, in which rat cortical CB_2 mRNA level was used as a reference to quantify the levels in other brain regions, whereas for rat testis CB_2 level was used as a reference to quantify CB_2 mRNA in peripheral tissues. For rat-specific rCB_{2C} and rCB_{2D} isoforms, the cortical CB_2 mRNA level was used as a reference for both brain and peripheral tissues.

π-helical conformation (bend helices) are also conserved (Filipek *et al*, 2003).

There are functional amino-acid substitutions between the mouse and rat receptors. The charged amino-acid substitutions between mCB_2R and rCB_2R are located in the proximity of the TMs (Figure 6c and d; IL1: R62Q, EL1: N103R, IL3: R218Q, and EL3: Q276K, the first letter for mouse and the second letter for rat) that might affect ligand binding and signal transduction. For example, Feng and Song (2003) have shown that the amino acids D3.49 and R3.50 in DRY motif of TM3 and A6.34 in TM6 of CB_2R are involved in ligand binding and signal transduction. Furthermore, the positively charged amino-acid substitution of C136R between rodent and primate CB_2R, respectively, is three amino acids downstream of the DRY domain and the substitution might change the ligand binding affinity between human and rat CB_2Rs.

The most striking difference of CB_2Rs between rat and mouse is that mCB_2R lacks the intracellular C-terminal 13 amino acids TGPGSRTPGCSNC of rCB_2R (348–360) as marked by single letters at the C-terminus of rCB_2R (Figure 6b and d). We searched The Eukaryotic Linear Motif Database and NetPhosK 2.0 using the intracellular C-terminal sequence (59 amino acids) of rCB_2R and found consensus motifs containing protein kinase C (PKC) phosphorylation site KSS (334–336, NetPhos score 0.995), G protein-coupled receptor kinase (GRK) phosphorylation site ETE (339–441, NetPhos score 0.663), and autophosphorylation site S352 (NetPhos score 0.962). The mCB_2R truncated 13 amino-acid sequence is located in the intrinsically disordered protein (IDP) motif KTTTGPGSRTPGCS (344–358, ELM prediction) (Dinkel *et al*, 2012) that allows more interactions with protein partners and modification sites. Therefore, the rCB_2R auophosphorylation site S352 (labeled in red in Figure 6b) and IDP motif do not exist in mCB_2R C-terminal intracellular domain.

DISCUSSION

One of the major findings in this study is that systemic administration of JWH133, a highly selective CB_2R agonist, produced different effects on i.v. cocaine self-administration in rats and mice. JWH133 dose-dependently inhibited cocaine self-administration under FR reinforcement in mice, but not in rats. Under PR reinforcement, JWH133 produced an increase in PR BP for cocaine self-administration in rats, but a decrease in PR BP for cocaine self-administration in mice. JWH133 may have relatively poor bioavailability because of rapid metabolism in liver after i.p. administration and/or rapid redistribution from plasma to fatty tissues after absorption. Therefore, higher drug doses of systemic JWH133 may be required to produce a similar inhibitory effect in rats as seen in mice. To explore this

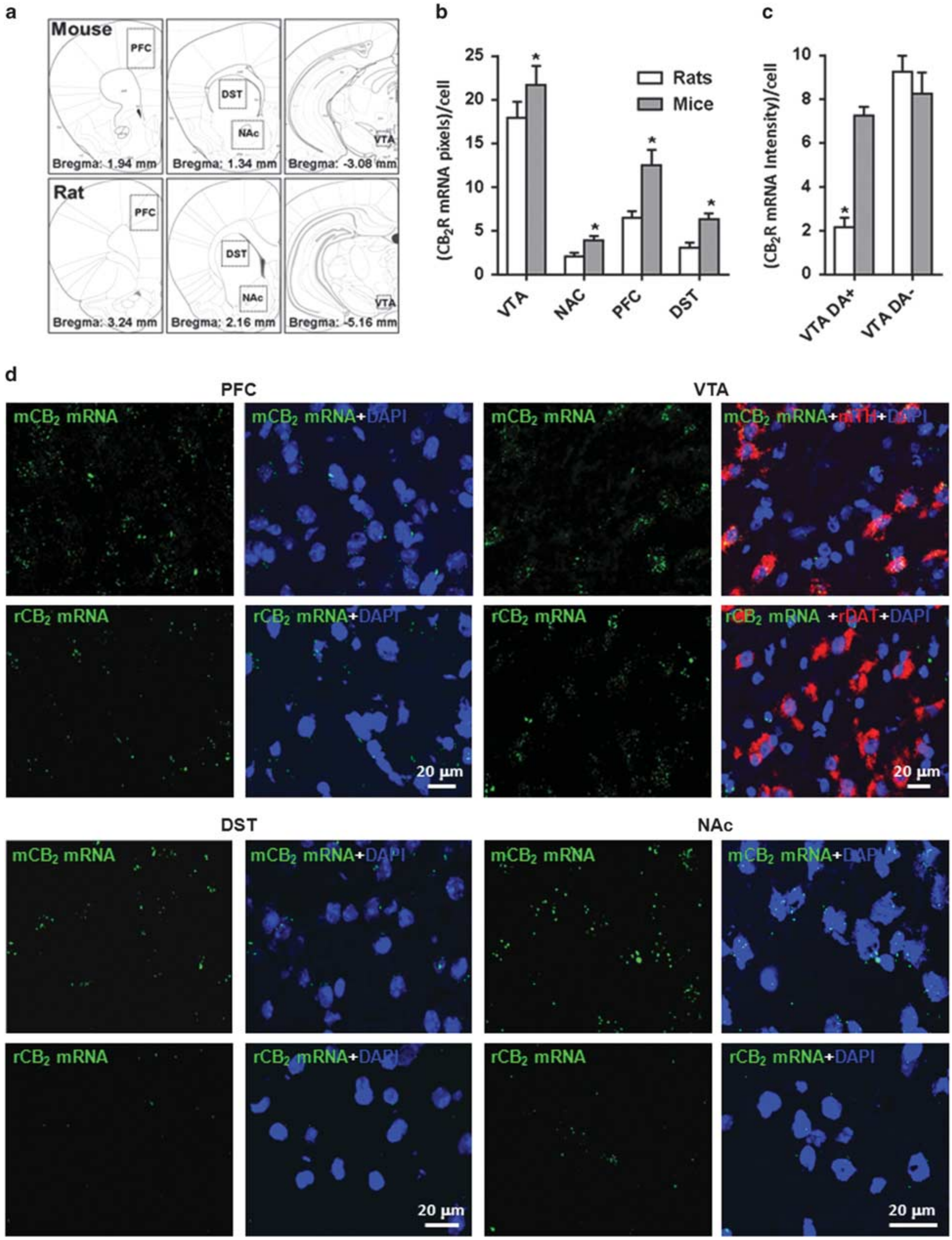

Figure 5 Brain CB_2 mRNA expression by RNAscope *in situ* hybridization (ISH) assays. (a) Brain section diagrams, illustrating the anatomic locations and the coordinates of PFC, DST, NAC, and VTA for the ISH images. (b, c) Quantification of CB_2R pixels or densities per cell in each brain region of mice and rats. (d) Representative RNAscope ISH microscope images of different brain regions. CB_2 mRNA signals are green, TH and DAT signals are red, and nuclear signals are blue (DAPI). Calibration bar is 20 μm. *$P<0.05$, compared with rats.

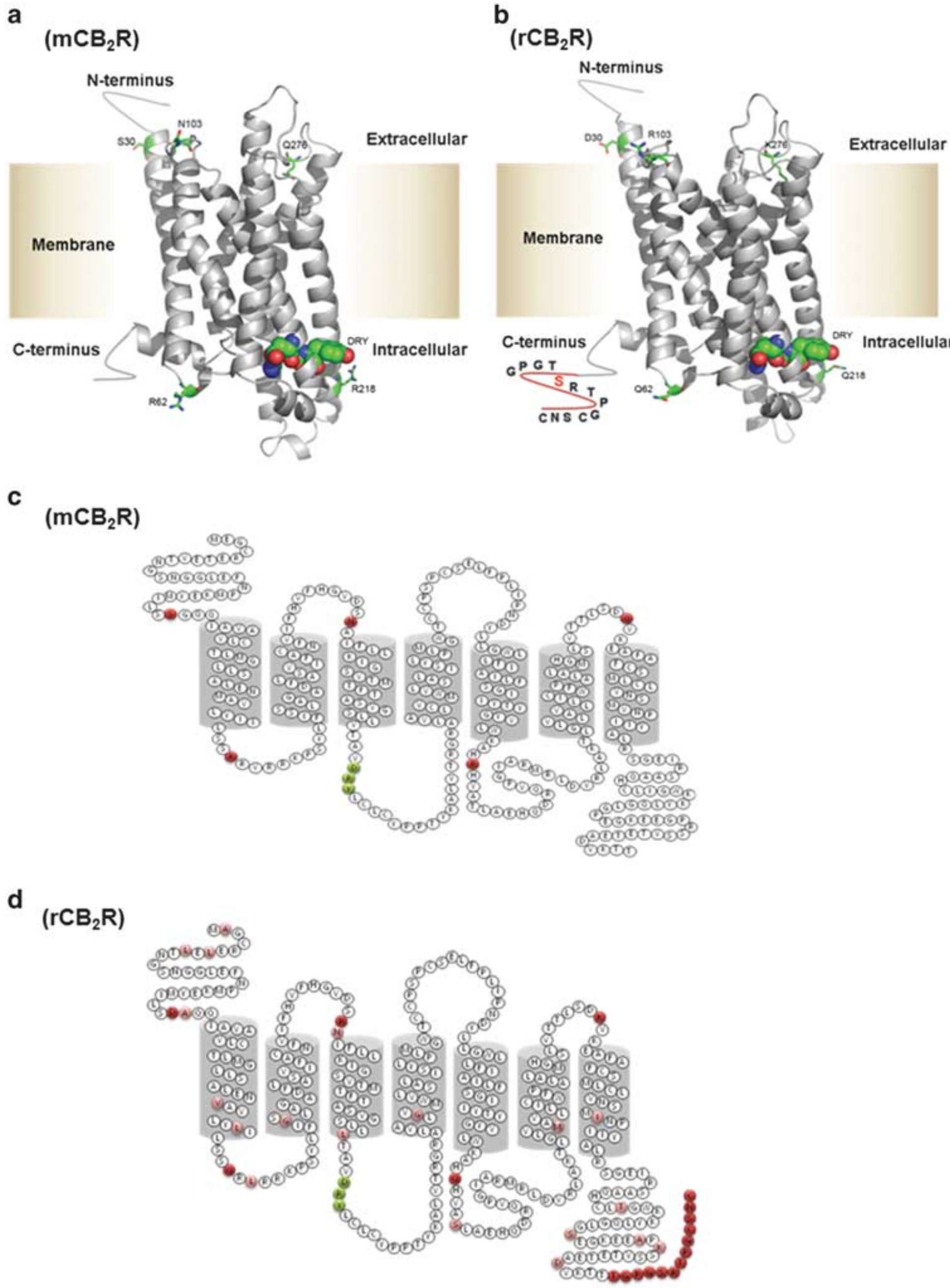

Figure 6 CB_2R 3D and 2D structures in rat and mouse. (a, b) *In silico* models of mCB_2R and rCB_2R 3D structures. (c, d) The corresponding amino-acid sequences of mCB_2R and rCB_2R. Ribbons represent seven transmembrane domains and bended lines represent intracellular and extracellular domains. The 'DRY' motif is indicated by colored balls. The charged amino-acid exchanges in the extracellular and the intracellular loops between mCB_2R and rCB_2R are marked by colored narrow lines labeled with amino-acid codes and numbers in the 3D models. The truncated 13 amino acids of mCB_2R are marked with single amino-acid code in the intracellular C-terminal domain of rCB_2R. The autophosphorylation site S352 is marked in red. The charged amino acid substitutions and the C-terminal truncation of mCB_2R are marked in the mCB_2R with dark red coloration (c, d) and other amino acid substitutions between mCB_2R and rCB_2R are marked in light red coloration (d).

hypothesis, JWH133 was delivered intranasally—a route by which the drug can directly enter the brain and bypass peripheral tissues. We found that JWH133 produced biphasic effects: low doses increased whereas a high dose inhibited PR cocaine self-administration in rats, suggesting that the increase in PR BP could be a compensatory response to a reduction in cocaine's rewarding efficacy after low doses of JWH133.

CB_2R gene structure and mRNA splicing are different in different species (Liu *et al*, 2009). This raises the possibility that CB_2Rs may have different regional and/or cellular distributions in brain between rats and mice and, therefore, may subserve different effects on motivation for drug taking and consumption. To explore this, we first carefully examined CB_2R gene or transcript expression in rats and mice by quantitative RT-PCR. We found four different rCB_2R mRNA isoforms. CB_{2A} and CB_{2B} are present in mice and rats, and CB_{2C} and CB_{2D} are present only in rats. It is unknown how these different CB_2R mRNA isoforms alter CB_2R expression in the brain. As the intact rCB_2R protein-coding region exists in the CB_{2A}, CB_{2B}, CB_{2C}, and CB_{2D} isoforms, we suggest that these four isoforms may encode or translate the same CB_2R in amino-acid sequence. The different sequences of 5′-UTR and 3′-UTR of the isoforms might alter brain regional and cell type-specific expression and mRNA stabilities. We note that the quantification of CB_2R isoform using qRT-PCR and agarose fragment analysis might not be accurate because of different probe designs and PCR cycles, respectively. We therefore used the RNAscope ISH assays to observe CB_2R mRNA expression patterns and quantify density in brain regions (VTA, NAC, PFC, and DST). We found that all of the examined mouse brain regions have more CB_2R mRNA than rat brain regions. The higher levels of CB_2R mRNA in mice might indicate a compensatory upregulation of mCB_2R mRNA because of the C-terminal truncation. We also noted that CB_2R mRNA levels in TH-positive DA neurons and TH-negative cells were very similar in mice, but were significantly lower in DAT-positive DA neurons than DAT-negative neurons in rats, suggesting species differences of CB_2R mRNA expression in DA neurons. This might in part contribute to the different behavioral responses to the agonist JWH133 seen in rats and mice.

We also examined the rCB_2R_{410} isoform (AF218846) that encodes 410 amino acids (Brown *et al*, 2002). The rCB_2R_{410} isoform is produced by an intraexonic splicing site upstream of the stop codon (nucleotide positions at FJ694960: 1198–2141, deletion of 943 bp), creating a frameshift that changes the C-terminal amino-acid sequence (Brown *et al*, 2002). However, in this study, we could not detect this frameshift isoform expression in rat brain and peripheral tissues using TaqMan probe and primers across the rCB_2R_{410} splicing site (data not shown). We detected the expected sizes of the rCB_2R_{360} and rCB_{2D} PCR fragments. Therefore, we concluded that the rCB_2R_{360} is a predominant isoform in rat. The rCB_{2D} isoform is caused by splicing site downstream of the stop codon (nucleotide positions at FJ694960: 1355–2141, deletion of 786 bp) that does not alter the C-terminal amino-acid sequence.

In addition to species differences in CB_2R gene splicing, we also found that CB_2Rs display significant species differences in amino acid sequences. There is 96% amino-acid homology between human and rhesus and 93% amino-acid homology between rat and mouse CB_2 receptors. Human CB_2R shares similar amino-acid homologies with mouse (82%) and rat (81%). However, the mCB_2R truncates the intracellular C-terminal 13 amino acids because of a premature stop codon that reduces mCB_2R to 347 amino acids instead of 360 amino acids (Liu *et al*, 2009). The truncated carboxyl-terminus of CB_2R contains a functional autophosphorylation site (Ser352) that may induce CB_2R internalization, an effect that is blocked by the CB_2R antagonist SR144528 (Bouaboula *et al*, 1999). The truncated C-terminus potentially contains the PDZ (postsynaptic density protein structural domain)-binding motif PGCSNC (355–360) (Bar-Shira and Chechik, 2013) that might position the rCB_2R in the postsynaptic density region as shown in hippocampus (Brusco *et al*, 2008a, b). Therefore, the postsynaptic signaling mechanisms of the CB_2R might differ from the presynaptic retrograde signaling of the CB_1R that is induced by depolarization-suppressing glutamate excitatory and GABA inhibitory neurotransmissions (Benarroch, 2007). However, synergistic actions between CB_1R and CB_2R might be implied by pre- and postsynaptic localizations of CB_1R in nucleus accumbens (Pickel *et al*, 2006). In comparison, rCB_2R_{360} (FJ694960) retains 360 amino acids (Liu *et al*, 2009) and an intact C-terminal intracellular sequence, including the autophosphorylation Ser352 site and the putative PDZ (355–360) domain, similar to the situation in the hCB_2R. The shortened C-terminus of mCB_2R might also change G-protein coupling for ligand-induced intracellular signal transduction. These findings suggest that the intracellular signal pathways underlying CB_2R signaling may be different in mouse and rat, and this may in part explain why JWH133 produces different effects on cocaine self-administration behavior in rats and mice. According to the similarity of the primary amino-acid sequences of the CB_2R, rCB_2Rs might be more relevant to hCB_2Rs, whereas according to the similarity of gene splicing pattern, mCB_2Rs might be more relevant to hCB_2Rs.

Importantly, CB_2Rs in different species also display different functional responses to the same ligands. For example, JWH133 is reported to be relatively selective for hCB_2Rs over rCB_2Rs, whereas the selective antagonist AM630 is more potent at rCB_2Rs than at hCB_2Rs, and the affinity of JWH133 for rCB_2Rs or mCB_2Rs is unknown (Huffman *et al*, 1999; Marriott *et al*, 2006). However, another CB_2R agonist, S-AM1241, shows clear differential affinity for rCB_2R (893 ± 58.5 nM) and mCB_2R (577 ± 58.4 nM), and regulation of cAMP levels for rCB_2R (EC50: $785 + 564$ nM) and mCB_2R (EC50: $2000 + 475$ nM) in rCB_2R- and mCB_2R-transfected CHO cells (Yao *et al*, 2006; Bingham *et al*, 2007), respectively. JWH133 might have differential affinities and cAMP effects at rCB_2Rs and mCB_2Rs as well. The endocannabinoids (anandamide and 2-arachidonyl glycerol) and WIN55212-2 are more hCB_2R selective, whereas CP55940 has similar affinity for both hCB_2Rs and rCB_2Rs (Griffin *et al*, 2000; Mukherjee *et al*, 2004; Yao *et al*, 2006). For computer modeling, we docked JWH133 to the active site of hCB_2R structure and predicted that JWH133 binding sites are located in TM2 (F87 and F91), TM3 (V113, W114, and F117), TM5 (L185, W194, and I198), TM6 (W258 and M265), and TM7 (S285). Although JWH133 binding sites are conserved in primates and rodents (Figure 7a and b), considerable differences in CB_2R amino-acid sequences and tertiary (3D) structures may underlie different receptor responses to various cannabinoid ligands in different species. Taken together, all these findings suggest that species differences in CB_2R gene and receptor expression in the brain may in part explain the different effects of JWH133 on cocaine self-administration described above.

During speciation, CB_1R evolved earlier than CB_2R. Chemotaxonomic and phylogenomic studies (McPartland, 2004) revealed that the genomes of non-chordate invertebrates do not encode CB_1R and CB_2R genes that are present in the genomes of vertebrates. Urochordates, a relative of vertebrates, encode only CB_1R and not CB_2R (Elphick, 2007). In non-chordate invertebrates lacking CB_1R and CB_2R genes, endocannabinoids, that is, anandamide and 2-arachidonyl glycerol, are found. These might act on

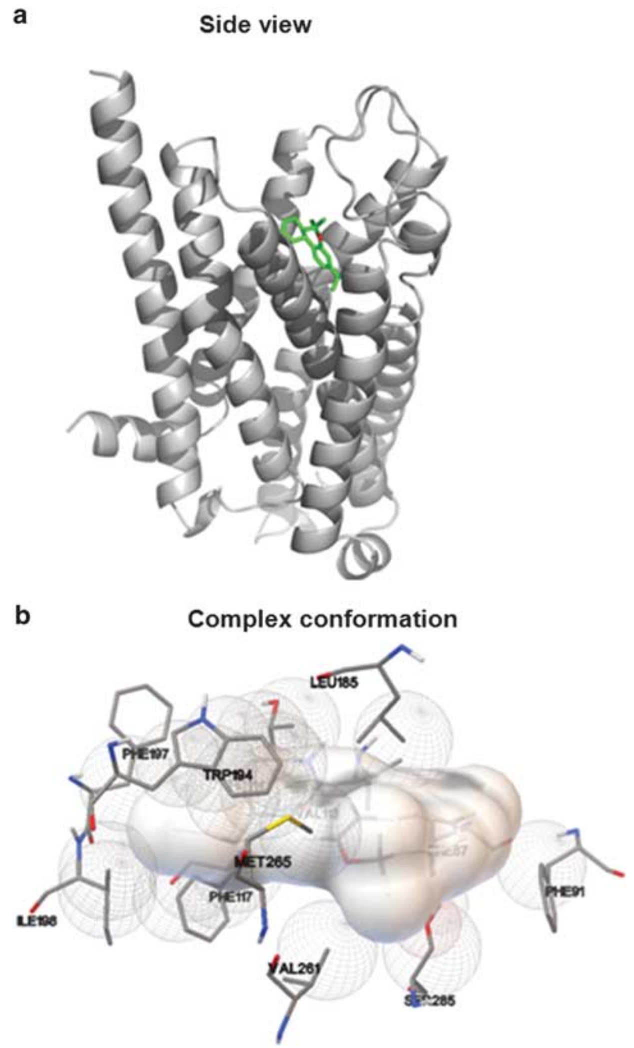

Figure 7 Computer models of JWH133 binding site of CB_2R. (a) JHW133 docking to the active site of hCB_2R. Green rings and lines represent JHW133 structure. (b) Complex conformations between JHW133 and hCB_2R. The JHW133 structure is represented by gray spheres and the amino-acid residues that contact with JHW133 are indicated by three-letter amino-acid symbols and numbers.

presynaptic transient receptor potential cation channel subfamily V member 1 (*Trpv1*) or on vanilloid receptor 1 (*VR1*) that evolved earlier than vertebrate cannabinoid receptors for regulation of invertebrate synaptic plasticity (Elphick, 2012). The enrichment of CB_1R in neuron and CB_2R in microglia might indicate commutative interactions of cannabinoids in neuron–glia circuitry (Cutando *et al*, 2013; Zhang *et al*, 2014b). The neuronal pre- and postsynaptic colocalization of CB_1R and CB_2R might imply cooperative signaling of cannabinoids (Brusco *et al*, 2008a; Reyes *et al*, 2009).

The existence of a premature stop codon might represent an effective regulation to change mCB_2R function by truncation of the C-terminal 13 amino acids. A mechanism also occurs in transient receptor potential cation channel (*TRPC2*) in hominoids and old-world monkeys that alters pheromone perception (Zhang and Webb, 2003), and in the taste receptor *TAS2R38* that changes the bitter taste perception of phenylthiocarbamide (PTC) in different mammalian species, including humans (Wooding, 2011). The CB_2R gene exhibits tissue- and species-specific alternative splicing because of *cis*-directed evolutionary changes in the nucleotide sequences of splicing sites of inter- and intraexon junctions (Barbosa-Morais *et al*, 2012). Within exon 2 of the rCB_2R gene, there is a potential 3′-splicing site (AG) with the consensus sequence of CAG/G that is changed to the nonconsensus sequence CAG/T in the corresponding mouse exon 2. Therefore, the rCB_2R exons 1–3 could be spliced together to form a new rCB_{2C} isoform. Tissue-specific gene expression is largely conserved in mammalian species but alternative splicing patterns are less conserved and often species specific (Merkin *et al*, 2012). The human hCB_2R gene lost rodent exon 1 and gained two exons further upstream during $\sim$75 million years of evolutionary branching from rodent (Modrek and Lee, 2003). Thus, promoter sequences and epigenetic regulation (Onaivi *et al*, 2012) of human CB_2R differ from rodents, as shown that hCB_{2A} is predominantly expressed in human testis (Liu *et al*, 2009; Onaivi *et al*, 2012). The emergence of alternative splicing sites of rat exon 2 and exon 3 created more rat rCB_2R transcript variants (4–5 isoforms) than those of mouse mCB_2R (2 isoforms) (Jorda *et al*, 2003; Koren *et al*, 2007). Human-specific alternative splicing is also present in hCB_1R (*CNR1*) gene in which intraexonic splicing of the coding exon produces different N-terminal domains that exhibit tissue-specific expression patterns (Shire *et al*, 1995). Therefore, alternative splicing plays a major role in mammalian evolution of cannabinoid system.

Conventional ISH is unable to detect CB_2R expression in nonstimulated rodent brain neurons because of lower sensitivity and specificity of unamplified probes (Wang *et al*, 2012). The ultrasensitive RNAscope ISH with amplified fluorescent probes detected more CB_2R mRNA signals in mouse brain than in rat brain (Figure 5), and rCB_2R protein was observed in postsynaptic regions (Brusco *et al*, 2008a, b). Differential brain CB_2R expression may also in part explain different effects of JWH133 on cocaine self-administration in rats and mice. This gene–behavior correlation is also observed in Lewis and Fischer 344 rat strains. For example, Lewis rats display lower PR BPs for cocaine self-administration, but have higher CB_2R expression in hippocampus than those of Fischer 344 rats who display higher PR BPs for cocaine self-administration (Rivera *et al*, 2013; Kosten *et al,* 2007), which agrees with our findings in mice and rats. Therefore, quantitative and qualitative changes in the mCB_2R gene might contribute to differential receptor responses to cocaine self-administration.

In conclusion, evolutionary changes in CB_2R including its coding sequences, splicing patterns, and gene regulatory elements might contribute in part to differential effects of CB_2R ligands on cocaine self-administration (Gamaleddin *et al*, 2012a; Ignatowska-Jankowska *et al*, 2013; Xi *et al*, 2011). With growing evidence that CB_2Rs play an important role in addiction, psychiatric, and neurological disorders, more studies are required to explore species differences in CB_2R gene expression and signal transduction. Proper selection of animal models is important in the development of effective CB_2R-based therapeutics for addiction and other psychiatric and neurological diseases in humans.

FUNDING AND DISCLOSURE

The authors declare no conflict of interest.

ACKNOWLEDGEMENTS

We gratefully acknowledge Dr Yavin Shaham, chief of the Behavioral Neuroscience Research Branch, Intramural Research Program, NIDA-NIH, for invaluable advice on statistical analysis. H-YZ, G-HB, XL, JL, Z-XX, ELG, and Q-RL are supported by the Intramural Research Program of the National Institute on Drug Abuse, National Institute of Health (NIDA-NIH). HQ is supported by the National Natural Science Foundation of China (31171270), and C-YL and S-JZ are supported by the National Key Basic Research Program of China (2012CB518004 and 2013CB531202). ESO acknowledges Guest Researcher support at NIDA-NIH and NIH grant DA032890.

REFERENCES

Adamczyk P, Miszkiel J, McCreary AC, Filip M, Papp M, Przegaliński E (2012). The effects of cannabinoid CB_1, CB_2 and vanilloid TRPV1 receptor antagonists on cocaine addictive behavior in rats. *Brain Res* **1444**: 45–54.

Al Mansouri S, Ojha S, Al Maamari E, Al Ameri M, Nurulain SM, Bahi A (2014). The cannabinoid receptor 2 agonist, β-caryophyllene, reduced voluntary alcohol intake and attenuated ethanol-induced place preference and sensitivity in mice. *Pharmacol Biochem Behav* **124**: 260–268.

Aracil-Fernández A, Trigo JM, García-Gutiérrez MS, Ortega-Álvaro A, Ternianov A, Navarro D *et al* (2012). Decreased cocaine motor sensitization and self-administration in mice overexpressing cannabinoid CB_2 receptors. *Neuropsychopharmacology* **37**: 1749–1763.

Arnold K, Bordoli L, Kopp J, Schwede T (2006). The SWISS-MODEL workspace: a web-based environment for protein structure homology modelling. *Bioinformatics* **22**: 195–201.

Atwood BK, Mackie K (2010). CB_2: a cannabinoid receptor with an identity crisis. *Br J Pharmacol* **160**: 467–479.

Bar-Shira O, Chechik G (2013). Predicting protein-protein interactions in the post synaptic density. *Mol Cell Neurosci* **56**: 128–139.

Barbosa-Morais NL, Irimia M, Pan Q, Xiong HY, Gueroussov S, Lee LJ *et al* (2012). The evolutionary landscape of alternative splicing in vertebrate species. *Science* **338**: 1587–1593.

Benarroch E (2007). Endocannabinoids in basal ganglia circuits: implications for Parkinson disease. *Neurology* **69**: 306–309.

Bingham B, Jones PG, Uveges AJ, Kotnis S, Lu P, Smith VA *et al* (2007). Species-specific in vitro pharmacological effects of the cannabinoid receptor 2 (CB_2) selective ligand AM1241 and its resolved enantiomers. *Br J Pharmacol* **151**: 1061–1070.

Blanco-Calvo E, Rivera P, Arrabal S, Vargas A, Pavón FJ, Serrano A *et al* (2014). Pharmacological blockade of either cannabinoid CB_1 or CB_2 receptors prevents both cocaine-induced conditioned locomotion and cocaine-induced reduction of cell proliferation in the hippocampus of adult male rat. *Front Integr Neurosci* **7**: 106.

Bouaboula M, Dussossoy D, Casellas P (1999). Regulation of peripheral cannabinoid receptor CB_2 phosphorylation by the inverse agonist SR 144528. Implications for receptor biological responses. *J Biol Chem* **274**: 20397–20405.

Brown SM, Wager-Miller J, Mackie K (2002). Cloning and molecular characterization of the rat CB_2 cannabinoid receptor. *Biochim Biophys Acta* **1576**: 255–264.

Brusco A, Tagliaferro P, Saez T, Onaivi ES (2008a). Postsynaptic localization of CB_2 cannabinoid receptors in the rat hippocampus. *Synapse* **62**: 944–949.

Brusco A, Tagliaferro PA, Saez T, Onaivi ES (2008b). Ultrastructural localization of neuronal brain CB_2 cannabinoid receptors. *Ann NY Acad Sci* **1139**: 450–457.

Buckley NE, McCoy KL, Mezey E, Bonner T, Zimmer A, Felder CC *et al* (2000). Immunomodulation by cannabinoids is absent in mice deficient for the cannabinoid CB_2 receptor. *Eur J Pharmacol* **396**: 141–149.

Callén L, Moreno E, Barroso-Chinea P, Moreno-Delgado D, Cortés A, Mallol J *et al* (2012). Cannabinoid receptors CB_1 and CB_2 form functional heteromers in brain. *J Biol Chem* **287**: 20851–20865.

Costantino HR, Illum L, Brandt G, Johnson PH, Quay SC (2007). Intranasal delivery: physicochemical and therapeutic aspects. *Int J Pharm* **337**: 1–24.

Cutando L, Busquets-Garcia A, Puighermanal E, Gomis-Gonzalez M, Delgado-Garcia JM, Gruart A *et al* (2013). Microglial activation underlies cerebellar deficits produced by repeated cannabis exposure. *J Clin Invest* **123**: 2816–2831.

den Boon FS, Chameau P, Schaafsma-Zhao Q, van Aken W, Bari M, Oddi S *et al* (2012). Excitability of prefrontal cortical pyramidal neurons is modulated by activation of intracellular type-2 cannabinoid receptors. *Proc Natl Acad Sci USA* **109**: 3534–3539.

Dinkel H, Michael S, Weatheritt RJ, Davey NE, Van Roey K, Altenberg B *et al* (2012). ELM–the database of eukaryotic linear motifs. *Nucleic Acids Res* **40(Database issue)**: D242–D251.

Elphick MR (2007). BfCBR: a cannabinoid receptor ortholog in the cephalochordate Branchiostoma floridae (Amphioxus). *Gene* **399**: 65–71.

Elphick MR (2012). The evolution and comparative neurobiology of endocannabinoid signalling. *Philos Trans R Soc Lond B Biol Sci* **367**: 3201–3215.

Feng W, Song ZH (2003). Effects of D3.49A, R3.50A, and A6.34E mutations on ligand binding and activation of the cannabinoid-2 (CB_2) receptor. *Biochem Pharmacol* **65**: 1077–1085.

Filipek S, Teller DC, Palczewski K, Stenkamp R (2003). The crystallographic model of rhodopsin and its use in studies of other G protein-coupled receptors. *Annu Rev Biophys Biomol Struct* **32**: 375–397.

Gamaleddin I, Wertheim C, Zhu AZ, Coen KM, Vemuri K, Makryannis A *et al* (2012a). Cannabinoid receptor stimulation increases motivation for nicotine and nicotine seeking. *Addict Biol* **17**: 47–61.

Gamaleddin I, Zvonok A, Makriyannis A, Goldberg SR, Le Foll B (2012b). Effects of a selective cannabinoid CB_2 agonist and antagonist on intravenous nicotine self administration and reinstatement of nicotine seeking. *PLoS One* **7**: e29900.

Garcia-Gutiérrez MS, Manzanares J (2011). Overexpression of CB_2 cannabinoid receptors decreased vulnerability to anxiety and impaired anxiolytic action of alprazolam in mice. *J Psychopharmacol* **25**: 111–120.

Gong J-P, Onaivi ES, Ishiguro H, Liu Q-R, Tagliaferro PA, Brusco A *et al* (2006). Cannabinoid CB_2 receptors: immunohistochemical localization in rat brain. *Brain Res* **1071**: 10–23.

Griffin G, Tao Q, Abood ME (2000). Cloning and pharmacological characterization of the rat CB(2) cannabinoid receptor. *J Pharmacol Exp Ther* **292**: 886–894.

Guex N, Peitsch MC (1997). SWISS-MODEL and the Swiss-PdbViewer: an environment for comparative protein modeling. *Electrophoresis* **18**: 2714–2723.

Gutiérrez MS, Ortega-Álvaro A, Busquets-García A, Pérez-Ortiz JM, Caltana L, Ricatti MJ *et al* (2013). Synaptic plasticity alterations associated with memory impairment induced by deletion of CB_2 cannabinoid receptors. *Neuropharmacology* **73**: 388–396.

Huffman JW, Liddle J, Yu S, Aung MM, Abood ME, Wiley JL *et al* (1999). 3-(1′,1′-Dimethylbutyl)-1-deoxy-delta8-THC and related compounds: synthesis of selective ligands for the CB_2 receptor. *Bioorg Med Chem* **7**: 2905–2914.

Ignatowska-Jankowska BM, Muldoon PP, Lichtman AH, Damaj MI (2013). The cannabinoid CB receptor is necessary for nicotine-conditioned place preference, but not other behavioral effects of nicotine in mice. *Psychopharmacology (Berl)* **229**: 591–601.

Illum L, Watts P, Fisher AN, Hinchcliffe M, Norbury H, Jabbal-Gill I *et al* (2002). Intranasal delivery of morphine. *J Pharmacol Exp Ther* **301**: 391–400.

Ishiguro H, Carpio O, Horiuchi Y, Shu A, Higuchi S, Schanz N *et al* (2010a). A nonsynonymous polymorphism in cannabinoid CB_2 receptor gene is associated with eating disorders in humans and food intake is modified in mice by its ligands. *Synapse* **64**: 92–96.

Ishiguro H, Horiuchi Y, Ishikawa M, Koga M, Imai K, Suzuki Y *et al* (2010b). Brain cannabinoid CB_2 receptor in schizophrenia. *Biol Psychiatry* **67**: 974–982.

Jorda MA, Rayman N, Valk P, De Wee E, Delwel R (2003). Identification, characterization, and function of a novel oncogene: the peripheral cannabinoid receptor Cb2. *Ann NY Acad Sci* **996**: 10–16.

Koren E, Lev-Maor G, Ast G (2007). The emergence of alternative 3' and 5' splice site exons from constitutive exons. *PLoS Comput Biol* **3**: e95.

Kosten TA, Zhang XY, Haile CN (2007). Strain differences in maintenance of cocaine self-administration and their relationship to novelty activity responses. *Behav Neusci* **121**: 380–388.

Lanciego JL, Barroso-Chinea P, Rico AJ, Conte-Perales L, Callen L, Roda E *et al* (2011). Expression of the mRNA coding the cannabinoid receptor 2 in the pallidal complex of *Macaca fascicularis*. *J Psychopharmacol* **25**: 97–104.

Liu Q-R, Pan CH, Hishimoto A, Li C-Y, Xi Z-X, Llorente-Berzal A *et al* (2009). Species differences in cannabinoid receptor 2 (*CNR_2* gene): identification of novel human and rodent CB_2 isoforms, differential tissue expression and regulation by cannabinoid receptor ligands. *Genes Brain Behav* **8**: 519–530.

Liu Q-R, Rubio FJ, Bossert JM, Marchant NJ, Fanous S, Hou X *et al* (2014). Detection of molecular alterations in methamphetamine-activated Fos-expressing neurons from a single rat dorsal striatum using fluorescence-activated cell sorting (FACS). *J Neurochem* **128**: 173–185.

Marriott KS, Huffman JW, Wiley JL, Martin BR (2006). Synthesis and pharmacology of 11-nor-1-methoxy-9-hydroxyhexahydro-cannabinols and 11-nor-1-deoxy-9-hydroxyhexahydrocannabinols: new selective ligands for the cannabinoid CB_2 receptor. *Bioorg Med Chem* **14**: 2386–2397.

Matsuda LA (1997). Molecular aspects of cannabinoid receptors. *Crit Rev Neurobiol* **11**: 143–166.

McPartland JM (2004). Phylogenomic and chemotaxonomic analysis of the endocannabinoid system. *Brain Res Brain Res Rev* **45**: 18–29.

Mechoulam R, Parker LA (2013). The endocannabinoid system and the brain. *Annu Rev Psychol* **64**: 21–47.

Mercier RW, Pei Y, Pandarinathan L, Janero DR, Zhang J, Makriyannis A (2010). hCB_2 ligand-interaction landscape: cysteine residues critical to biarylpyrazole antagonist binding motif and receptor modulation. *Chem Biol* **17**: 1132–1142.

Merkin J, Russell C, Chen P, Burge CB (2012). Evolutionary dynamics of gene and isoform regulation in Mammalian tissues. *Science* **338**: 1593–1599.

Modrek B, Lee CJ (2003). Alternative splicing in the human, mouse and rat genomes is associated with an increased frequency of exon creation and/or loss. *Nat Genet* **34**: 177–180.

Morgan NH, Stanford IM, Woodhall GL (2009). Functional CB_2 type cannabinoid receptors at CNS synapses. *Neuropharmacology* **57**: 356–368.

Mukherjee S, Adams M, Whiteaker K, Daza A, Kage K, Cassar S *et al* (2004). Species comparison and pharmacological characterization of rat and human CB_2 cannabinoid receptors. *Eur J Pharmacol* **505**: 1–9.

Navarrete F, Rodríguez-Arias M, Martín-García E, Navarro D, García-Gutiérrez MS, Aguilar MA *et al* (2013). Role of CB_2 cannabinoid receptors in the rewarding, reinforcing, and physical effects of nicotine. *Neuropsychopharmacology* **38**: 2515–2524.

Onaivi ES, Ishiguro H, Gong J-P, Patel S, Meozzi PA, Myers L *et al* (2008). Functional expression of brain neuronal CB_2 cannabinoid receptors are involved in the effects of drugs of abuse and in depression. *Ann NY Acad Sci* **1139**: 434–449.

Onaivi ES, Ishiguro H, Gu S, Liu Q-R (2012). CNS effects of CB_2 cannabinoid receptors: beyond neuro-immuno-cannabinoid activity. *J Psychopharmacol* **26**: 92–103.

Pickel VM, Chan J, Kearn CS, Mackie K (2006). Targeting dopamine D_2 and cannabinoid-1 CB_1 receptors in rat nucleus accumbens. *J Comp Neurol* **495**: 299–313.

Reyes BA, Rosario JC, Piana PM, Van Bockstaele EJ (2009). Cannabinoid modulation of cortical adrenergic receptors and transporters. *J Neurosci Res* **87**: 3671–3678.

Rivera P, Miguens M, Coria SM, Rubio L, Higuera-Matas A, Bermudez-Silva FJ *et al* (2013). Cocaine self-administration differentially modulates the expression of endogenous cannabinoid system-related proteins in the hippocampus of Lewis vs. Fischer 344 rats. *Int J Neuropsychopharmacol* **16**: 1277–1293.

Rosenbaum DM, Rasmussen SG, Kobilka BK (2009). The structure and function of G-protein-coupled receptors. *Nature* **459**: 356–363.

Schwede T, Kopp J, Guex N, Peitsch MC (2003). SWISS-MODEL: an automated protein homology-modeling server. *Nucleic Acids Res* **31**: 3381–3385.

Shire D, Carillon C, Kaghad M, Calandra B, Rinaldi-Carmona M, Le Fur G *et al* (1995). An amino-terminal variant of the central cannabinoid receptor resulting from alternative splicing. *J Biol Chem* **270**: 3726–3731.

Song R, Zhang HY, Li X, Bi GH, Gardner EL, Xi ZX (2012). Increased vulnerability to cocaine in mice lacking dopamine D3 receptors. *Proc Natl Acad Sci USA* **109**: 17675–17680.

Song ZH, Feng W (2002). Absence of a conserved proline and presence of a conserved tyrosine in the CB_2 cannabinoid receptor are crucial for its function. *FEBS Lett* **531**: 290–294.

Suárez J, Llorente R, Romero-Zerbo SY, Mateos B, Bermúdez-Silva FJ, de Fonseca FR *et al* (2009). Early maternal deprivation induces gender-dependent changes on the expression of hippocampal CB_1 and CB_2 cannabinoid receptors of neonatal rats. *Hippocampus* **19**: 623–632.

Tao Q, McAllister SD, Andreassi J, Nowell KW, Cabral GA, Hurst DP *et al* (1999). Role of a conserved lysine residue in the peripheral cannabinoid receptor CB_2: evidence for subtype specificity. *Mol Pharmacol* **55**: 605–613.

Tubbs RR, Wang H, Wang Z, Minca EC, Portier BP, Gruver AM *et al* (2013). Ultrasensitive RNA in situ hybridization for detection of restricted clonal expression of low-abundance immunoglobulin light chain mRNA in B-cell lymphoproliferative disorders. *Am J Clin Pathol* **140**: 736–746.

Van Sickle MD, Duncan M, Kingsley PJ, Mouihate A, Urbani P, Mackie K *et al* (2005). Identification and functional characterization of brainstem cannabinoid CB_2 receptors. *Science* **310**: 329–332.

Vinckenbosch N, Dupanloup I, Kaessmann H (2006). Evolutionary fate of retroposed gene copies in the human genome. *Proc Natl Acad Sci USA* **103**: 3220–3225.

Wang F, Flanagan J, Su N, Wang L-C, Bui S, Nielson A *et al* (2012). RNAscope: a novel *in situ* RNA analysis platform for formalin-fixed, paraffin-embedded tissues. *J Mol Diagn* **14**: 22–29.

Wooding S (2011). Signatures of natural selection in a primate bitter taste receptor. *J Mol Evol* **73**: 257–265.

Xi Z-X, Gilbert JG, Pak AC, Ashby CR Jr., Heidbreder CA, Gardner EL (2005). Selective dopamine D_3 receptor antagonism by SB-277011A attenuates cocaine reinforcement as assessed by progressive-ratio and variable-cost-variable-payoff fixed-ratio cocaine self-administration in rats. *Eur J Neurosci* **21**: 3427–3438.

Xi Z-X, Peng X-Q, Li X, Song R, Zhang H-Y, Liu Q-R *et al* (2011). Brain cannabinoid CB receptors modulate cocaine's actions in mice. *Nat Neurosci* **14**: 1160–1166.
Yao BB, Mukherjee S, Fan Y, Garrison TR, Daza AV, Grayson GK *et al* (2006). In vitro pharmacological characterization of AM1241: a protean agonist at the cannabinoid CB_2 receptor? *Br J Pharmacol* **149**: 145–154.
Zhang J, Webb DM (2003). Evolutionary deterioration of the vomeronasal pheromone transduction pathway in catarrhine primates. *Proc Natl Acad Sci USA* **100**: 8337–8341.
Zhang S-J, Liu C-J, Shi M, Kong L, Chen J-Y, Zhou W-Z *et al* (2013). RhesusBase: a knowledgebase for the monkey research community. *Nucleic Acids Res* **41(Database issue)**: D892–D905.
Zhang S-J, Liu C-J, Yu P, Zhong X, Chen J-Y, Yang X *et al* (2014a). Evolutionary interrogation of human biology in well-annotated genomic framework of rhesus macaque. *Mol Biol Evol* **31**: 1309–1324.
Zhang Y, Chen K, Sloan SA, Bennett ML, Scholze AR, O'Keeffe S *et al* (2014b). An RNA-sequencing transcriptome and splicing database of glia, neurons, and vascular cells of the cerebral cortex. *J Neurosci* **34**: 11929–11947.